Biophysical Journal Volume 106 April 2014 1528–1536

Interactions and Tradeoffs Between Cell Recruitment, Proliferation, and Differentiation Affect CNS Regeneration

William R. Holmes and Qing Nie*
Center for Mathematical and Computational Biology, Center for Complex Biological Systems, Department of Mathematics, University of California, Irvine, California

ABSTRACT Regeneration of central nervous system (CNS) lesions requires movement of progenitor cells and production of their differentiated progeny. Although damage to the CNS clearly promotes these two processes, the interplay between these complex events and how it affects a response remains elusive. Here, we use spatial stochastic modeling to show that tradeoffs arise between production and recruitment during regeneration. Proper spatial control of cell cycle timing can mitigate these tradeoffs, maximizing recruitment, improving infiltration into the lesion, and reducing wasteful production outside of it. Feedback regulation of cell lineage dynamics alone however leads to spatial defects in cell recruitment, suggesting a novel, to our knowledge, hypothesis for the aggregation of cells to the periphery of a lesion in multiple sclerosis. Interestingly, stronger chemotaxis does not correct this aggregation and instead, substantial random cell motions near the site of the lesion are required to improve CNS regeneration.

INTRODUCTION

Given the prevalence and cost of chronic wounds, considerable efforts have been directed at understanding the choreographed events set in motion by damage that lead to repair and regeneration. Although wounds of the epidermis are possibly the best studied, lesions of the central nervous system (CNS) are arguably the most devastating and irreparable. Common causes include damage from external sources and neurological disorders such as multiple sclerosis (MS), which affects >2 million worldwide and 300,000 in the United States (according to National Institute of Neurological Disorders and Stroke (NINDS)).

The pathology of CNS injury of course depends on its source, but one broad class referred to as demyelinating diseases is characterized by the loss of oligodendrocytes (OLGs) (1–3). The cells, which support and insulate neurons, are vital for neural function and their loss leads to substantial neurological impairment. In fact, the death of these cells, rather than neurons themselves, is the primary source of impairment in MS. Their replacement is thus a necessary component of regeneration. Unfortunately, in many cases the progenitor cells (OPCs) that give rise to OLGs are also lost or rendered incapable of producing healthy progeny. Matters are further complicated by the fact that OLGs are not themselves motile and quickly undergo apoptosis in the absence of axonal contact (4,5). Thus, at a minimum, a proper response requires both recruitment of progenitors to the site of a lesion, and their differentiation to replace those lost to damage (6–8). Each of these processes must be properly regulated by inflammatory factors (9) or other signals.

Numerous investigations have cataloged the effects of various inflammatory ligands on the dynamics of neural stem/progenitor cell production and differentiation in the CNS (9–12). Others have investigated the processes that mediate recruitment (13–16). These efforts have largely ignored the fact that the two occur at the same time and are likely regulated by the same chemical factors. Spatial aspects of epidermal regeneration and tumor development, both of which involve complex spatiotemporal organization, are also the subject of intense research. However, these tissues are typically continuously self-renewing, whereas CNS tissue is best described as quiescent, because neurons and myelinating OLGs stabilize each other (4,5). This suggests different control goals and mechanisms in CNS regeneration.

Modeling has proved to be an effective tool for investigating 1), the feedbacks that control lineage commitment and regeneration (17–21) and 2), the role of those feedbacks in homeostasis (22–24). These have however been nonspatial investigations and considered only temporal dynamics. Spatial models of epidermal regeneration (25–27) have yielded important insights into the role of spatial organization but not considered the role of stem/progenitor cells. Other models have investigated stem cell dynamics in tumor development (28,29) or the role of chemokine-mediated stem cell dynamics during epidermal development (30,31). These have however assumed cell movements are purely passive and driven by proliferative pressures.

Understanding regeneration failure requires consideration of the interplay between temporal dynamics of lineage commitment and spatial dynamics of cell recruitment. Are these processes regulated independently or in a coordinated fashion? When, where, and how fast should proliferation occur? Should proliferation or differentiation be promoted

Submitted October 18, 2013, and accepted for publication February 6, 2014.

*Correspondence: qnie@math.uci.edu

Editor: Stanislav Shvartsman.

0006-3495/14/04/1528/9 $2.00

http://dx.doi.org/10.1016/j.bpj.2014.02.010

during the recruitment process? Does a speedup cell cycle progression always accelerate regeneration?

We use spatial stochastic modeling techniques to address these questions and characterize strategies for spatially regulating linage dynamics when chemotactic recruitment is required. The interaction between the two introduces unexpected tradeoffs. In particular, different strategies are required for efficient cell recruitment at early and late times after damage. Furthermore, these strategies lead to poor infiltration of cells to the interior of a lesion and wasteful production of cells beyond it that will quickly undergo apoptosis. These can be mitigated by limiting any speedup of the cell cycle to a local region near the lesion. This however still leads to spatial defects in recruitment that can only be improved by regulating motility itself.

MATERIALS AND METHODS

A verbal model for the dynamics of a generic renewable tissue is schematically outlined in Fig. 1, *a* and *b*, where it is assumed progenitors (P) have the following properties:

1. They are produced from a pool of stem cells (S) at constant rate r.
2. Each new P can divide at most n times before differentiating (D) (they are transiently amplifying). In vitro data for OPCs suggest $n \approx 8$ (32,33).
3. At any stage a progenitor can differentiate prematurely with probability $1 - q_i$.
4. Each progenitor can spend an extended period of time in quiescence (G0). This is encoded in a net cell cycle time τ that has two components, an active time τ_a associated with differentiation/division, and a quiescence time τ_q that the cell spends in G0.
5. Progenitors can chemotax to the site of a lesion, whereas differentiated cells are essentially nonmotile.

Motility properties are motivated by known dynamics of cells of the OLG line (14,34) where progenitors are mobile and differentiated cells are not. Stem/progenitor lineage dynamics, schematically outlined in Fig. 1, are canonical (see (18,19) for example). In contrast to previous investigations however, we will be primarily concerned with how the need for recruitment coupled with transient amplification affect regeneration responses. Because progenitor dynamics are our primary focus, we do not explicitly model dynamics of the stem cell population but rather assume it provides a constant, spatially uniform source of progenitors in healthy tissue.

Two primary questions dictate the formalism we use to translate this verbal model into a mathematical model. 1), How is a healthy steady-state cell density maintained? This has been addressed in relation to continuously self-renewing tissues such as the olfactory epithelium (18,19). However, the lack of regularly scheduled programmed cell death distinguishes a quiescent tissue from the more prototypically studied epithelial type tissue, suggesting different control goals and mechanisms. 2), What adjustments to intrinsic cell proliferative properties are required to elicit a good response to damage?

A nonspatial deterministic model (see the Supporting Material text, section 1) encoding the dynamics in Fig. 1 *a* is used to describe dynamics of healthy tissue. The resulting steady state is

$$P_s^{tot} = rS\tau\frac{1-(2q)^{n+1}}{1-2q}, \quad D_s = \frac{rS}{2d}\left(1+\frac{1-(2q)^{n+1}}{1-2q}\right), \quad (1)$$

where P_s^{tot} is the progenitor density summed over the different progenitor stages (P^i) (which are not individually observable), D_s is the terminally differentiated (TD) density, and for simplicity proliferation probabilities are assumed to be independent of stage so that $q_i = q$ for all i (because individual states are not distinguishable experimentally).

Damaged tissue is however not at steady state and is spatially heterogeneous. Furthermore, cell densities in the CNS are very low requiring consideration of stochastic effects. For these reasons a spatial stochastic model is used to describe dynamics of repair. Lineage dynamics are assumed to be stochastic and cell motions are modeled by Langevin dynamics with w describing a chemotactic sensitivity and σ the strength of random Brownian motions. We consider a circular lesion of radius r_0 in two spatial dimensions devoid of functional TD cells/progenitors and surrounded by unaffected healthy tissue. The range of influence of the lesion (mediated by a diffusable ligand for example) is assumed to extend to a radius r_M from the center so that cells can be recruited from an annular region (Ω) spanning these two radii.

Within this framework we consider two strategies for spatially regulating proliferation properties (cell cycle and proliferation probability). First, these properties (q, τ) along with chemotaxis are coregulated so that the lesion influences each to roughly the same spatial extent. Second, they are separately regulated (by different ligands for example) and the lesion can influence each to different spatial extents. In both cases, we assume an explicit dependence of these properties on space rather than model the spread of ligands, which are likely at steady state on the timescales of interest. See the next section for further details.

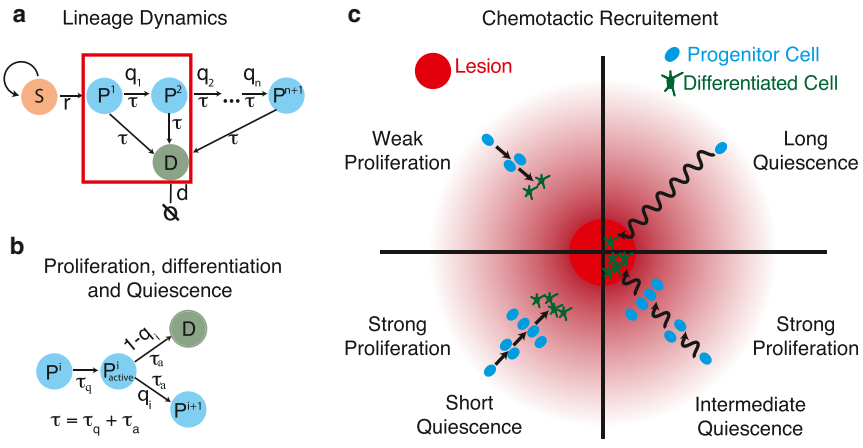

FIGURE 1 Schematic depiction of spatiotemporal progenitor dynamics during regeneration. (*Panel a*) Depiction of the multistage lineage dynamics involving self-renewing stem cells (S) that give rise to transiently amplifying progenitor cells (P), which in turn differentiate to form terminally differentiated cells (D). τ is an intrinsic cell cycle length, whereas q is a probability of dividing versus differentiating. (*Panel b*) A breakdown of one cycle of lineage progression (*red box in panel a*, for example). Each initially quiescent progenitor is assumed to exit quiescence with time constant τ_q, and then make the choice to either divide or differentiate, which we assume take the same amount of time for simplicity. (*Panel c*) Schematic of chemotactic recruitment scenarios with different proliferative control. To see this figure in color, go online.

Stochastic model and simulation

To describe the transient dynamics of regeneration, we used a discrete, spatial stochastic model of the verbal model described previously. Each cell is a discrete object whose lineage dynamics are stochastic. The net cell cycle length is assumed to be exponentially distributed with mean value τ. Upon exiting quiescence, either differentiation or proliferation occurs instantaneously with probabilities $1 - q_i$ and q_i, respectively. Because cell movement is important, chemotaxis and random motion are considered as well. Complexities of shape or mechanical cell-cell interactions are not described and cells are instead considered to be point entities. Langevin dynamics for the position ($\vec{r_i}$) of each cell are used to describe their motions

$$d\vec{r_i} = w\nabla C + \sqrt{2\sigma}\eta(t). \tag{2}$$

Here, ∇C is the gradient of a chemotactic signal and η is the standard Gaussian white noise term (temporally uncorrelated). The chemotactic sensitivity is taken to be ligand independent with $w = 0.02$ mm/h. The in silico lesion is radially symmetric and the chemotactic gradient piecewise constant with $\nabla C = -K\vec{r_i}/|\vec{r_i}|$ where r_i is the radial location of cell i,

$$K = \begin{cases} 0.1, & r<r_0 \\ 1, & r_0<r<r_M \\ 0, & r_M<r, \end{cases} \tag{3}$$

r_0 is the radius of the lesion, and r_M is the radius at which the chemotactic signal becomes insufficient to direct motion. Reduction of the chemotactic tendency in the interior of the lesion is assumed to come from one or both of two sources: 1), saturation of the chemotactic signal, or 2), loss of signal fidelity (reduced slope), which also degrades direction sensing.

Rather than implement a full spatial stochastic SSA algorithm, we decouple lineage and motility dynamics. Positional vectors are updated according to

$$\vec{r_i}(t+dt) = \vec{r_i}(t) + w\nabla C dt + \sqrt{2\sigma dt}\eta(t). \tag{4}$$

During this time interval a transition to the active phase is assumed to occur with probability

$$p = 1 - \exp\left(-\frac{dt}{\tau}\right). \tag{5}$$

A time interval of $dt = 1$ h was found to be sufficient (e.g., dynamics do not change with smaller dt). This is small enough that the probability of two events occurring is extremely small and can be neglected. Cells that enter the active phase are then chosen to divide with probability q_i or differentiate with probability $1 - q_i$. Both position and state are updated at the end of each time step, any new cells are initialized at the appropriate location, and the process is iterated for subsequent time intervals until the final time T is reached.

Rather than introduce a diffusable ligand, it is assumed q and τ depend directly on distance from the lesion. For analytical simplicity, a step function dependence is assumed in Fig. 2 where q, τ drop from their assigned values to q^h, τ^h at a distance r_M from the lesion. Where stochastic simulations are used, a continuous Michaelis-Menten dependence on space is assumed.

$$\tau = \tau^w - c\frac{r-r_0}{r_{crit}+(r-r_0)}, \quad q = q^w - c\frac{r-r_0}{r_{crit}+(r-r_0)}, \tag{6}$$

where (τ^w, q^w) are the values inside the lesion, r_{crit} is the distance at which the median response (or EC50) occurs, and c is a constant ensuring continuity at the boundary between affected and healthy tissue (radius $= r_M$) where values $q^h \approx 0.25$ and $\tau^h \approx 9$ days are assumed (see the Supporting Material text, section 2 for the computation of these values and Results for a discussion of their implications).

Properties of an effective regeneration response

We use this modeling framework to assess the effectiveness of different regulatory strategies at mounting a repair response. A good response requires three things: i), A sufficient number of differentiated TD cells should be delivered to the site of damage; ii), those cells infiltrate the entire lesion; and iii), the number of unnecessary differentiated cells produced in healthy tissue is low. The importance of i) and ii) is clear, whereas iii) is motivated by the quiescent nature of CNS tissue and the desire to reduce unnecessary production of TD cells fated for death. The relative importance of each of these is however subjective and depends on context. Therefore, rather than define a single measure of how effective a response is, we will define one for each property. R_p and R_c are defined as the number of TDs recruited to the lesion periphery and core, respectively, R_e the number produced in healthy tissue, and $R_t = R_p + R_c$. These measures will be dependent on the lesion structure (r_0, r_M), cell dynamics (q_i, τ, w, n), and the desired time (T) of a response.

These recruitment measures ($R_{p,c,e}$) are stochastic in nature and in general an ensemble simulation approach (35) is required to compute an expected or mean response. This can require days of computation (on high performance desktops) when different parameters and strategies (i.e., values for q_i, τ, n) are being explored (as in Fig. 2). When motions are deterministic ($\sigma = 0$) and susceptibility of cells to the lesions influence is ultrasensitive, the expected value of R_t can be computed directly. Consider a single progenitor initially located at position x. Define $N_i(q, T)$ as the expected number of TD cells produced by a single progenitor by time T and $L_i(w, \tau, n, x, T)$ the likelihood of any one of those reaching the lesion by that time. Therefore, the expected number of cells recruited by time T is

$$R_t = \delta\sum_{i=1}^{n+1}\int_{\Omega} N_i(q,T)L_i(w,\tau,n,x,T)dx, \tag{7}$$

where δ is the progenitor density in the region Ω of healthy tissue. N_i and L_i can be computed explicitly and in the case of the circular lesion here, the integral can be computed analytically (see the Supporting Material text, section 3).

RESULTS

Promoting differentiation rather than slowing cell cycle progression limits TD production

It is evident from the lack of dependence of the steady-state total TD death rate ($D_s^{flux} = d\,D_s$, in Eq. 1) on τ that cell cycle control alone cannot modulate cell densities or the production rate of TD cells at steady state. How then is this flux controlled? We use Eq. 1 along with cell density and proliferation assay data to infer cell cycle length (τ) and proliferation probability (q) at steady state. Typical proliferation assays make use of the cumulative S-phase marker BrdU that is incorporated during DNA replication and remains present through subsequent cell divisions. However, Ki67 expression type data marks all active phases of proliferation (G1, S, G2, and M phases) but not the quiescent G0 phase (37), making it ideal to

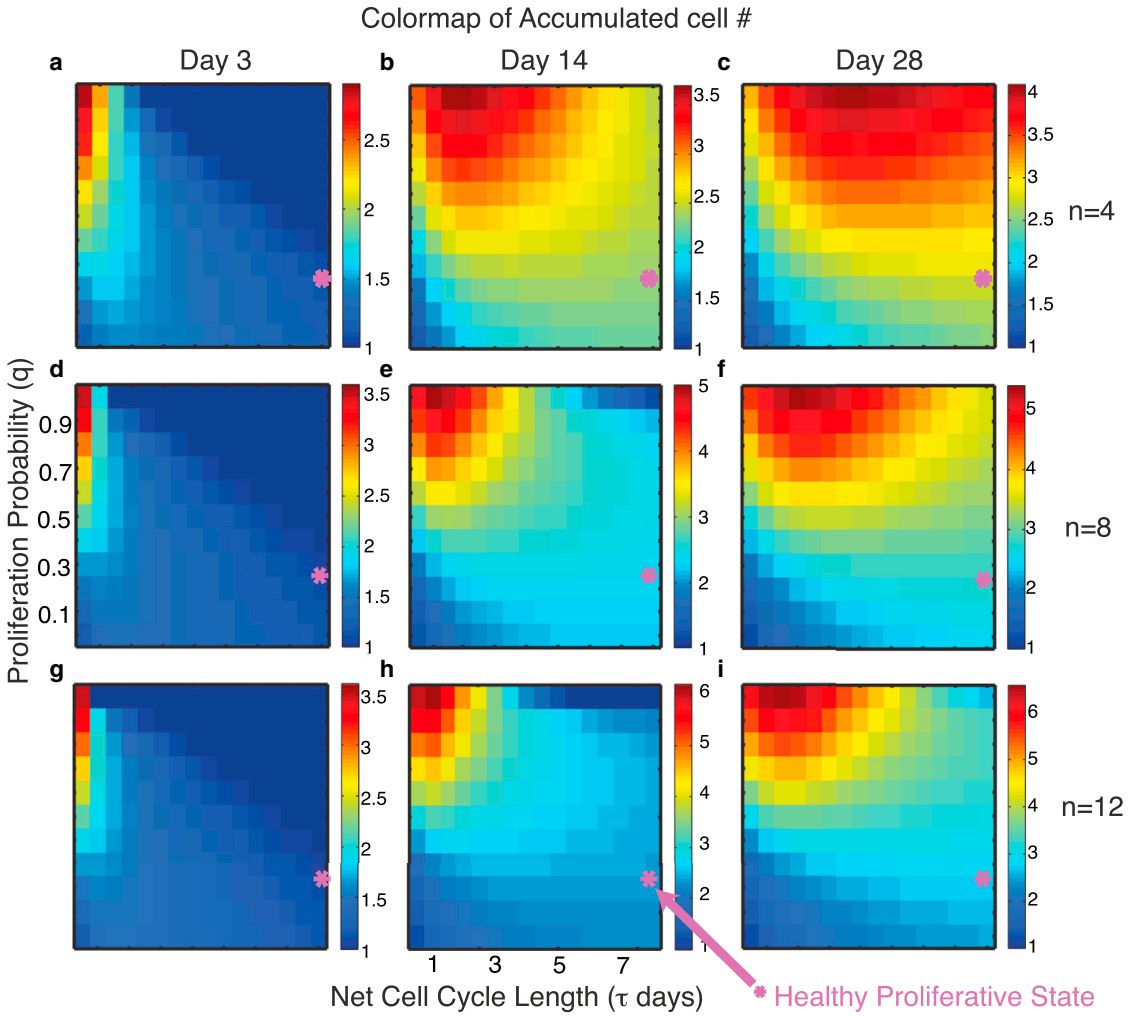

FIGURE 2 Optimal lineage dynamics for the recruitment response depend on n and T. Heat map representing the number of TD cells drawn to an in silico lesion in two spatial dimensions under different parametric conditions. Each panel quantifies the number of cells recruited to the lesion (depicted in Fig. 1 *c*) as a function of q, τ. Each column indicates the cumulative number of cells recruited by a specific time ($T = 3, 14, 28$), whereas each row indicates results for different values of the proliferative restriction ($n = 4, 8, 12$). Base 10 logarithm of cell numbers R_t (computed using Eq. 7) is reported. Purple stars depict the state of progenitors (e.g., the values of q^h, τ^h) in the healthy CNS (see Results and Supporting Material text, section 2). The domain is the 2D plane with a $r_0 =$ 5 mm radius circular lesion (initially devoid of TD and progenitor cells) surrounded by a region of healthy tissue (see Fig. 1 *c* for *schematic*). The range of influence of the damage extends to a radius $r_M = 15$ mm and the initial cell density is 5 cells/mm^2 (this lower density is used to reduce computational time in simulations later). The chemotactic velocity is $w = 0.02$ mm/h. To see this figure in color, go online.

estimate the fraction of cells (α) in the process of proliferating at a given time.

We make two specific assumptions about the differentiation/proliferation processes. First, differentiation occurs through morphological change rather than asymmetric division (38). Therefore, differentiation and proliferation are mutually exclusive events and differentiation is not marked by Ki67 expression. Second, both are considered active processes whose average time to completion is described by the time constant τ_a. These constraints can be used to estimate q and τ (see the Supporting Material text, section 2 for further detail)

$$q \approx \frac{\alpha P_s^{tot}}{\alpha P_s^{tot} + d\tau_a D_s}, \quad \tau = \frac{q\tau_a}{\alpha}. \tag{8}$$

Time course observations can of course be used to determine these parameters. The benefit of this approach however is that it requires data only at a single time point, for which in vivo data is more accessible.

Quantitative data from mouse CNS observations (4,36,39) combined with this result show that for OPCs in healthy tissue, $q \approx 0.26$ and $\tau \approx 8.8$ (see the Supporting Material text, section 2). So there is a strong bias toward differentiation and OPCs spends on the order of 1 week in G0. This is a surprising strategy given that in principle, by arresting the stem or progenitor population in G0 or substantially slowing the cell cycle, wasteful flux of TDs could be minimized. This is however not the case and the progenitor cell cycle is fast relative to the very long lifetime of differentiated OLGs. Instead, a strong tendency to differentiate is

responsible for reducing the flux of TD cells. In retrospect though, this is sensible because differentiation occurs at the expense of proliferation. Thus, promoting differentiation early avoids excess proliferation.

We note that the expression for q in Eq. 8 is an approximation. As a result it has a limited range of validity. In particular, it is only valid provided the resulting value of $q \lesssim 0.4$. The technical reason for this requirement is discussed in the Supporting Material text, section 2. Intuitively, in this regime the proliferation process is effectively truncated because most cells differentiate before reaching the later progenitor stages. This simplifies matters and results in this estimate being independent of the proliferative restriction n. Further discussion, along with a more general, exact expression for q without these limitations are provided in the Supporting Material text. We also note that in practice, total population levels become large quickly when $q > 0.5$. Therefore, at a healthy steady state, a practical maximum on the net cell cycle length is $\tau = \tau_a/(2\alpha)$, which is between 2 and 4 weeks for OPCs (assuming $\tau_a = 1$–2 days). Thus, extremely long quiescent periods do not appear to be responsible for slowing cell production in the healthy CNS.

Intertemporal tradeoff between strong early and late time responses

How can damage-induced adjustments to quiescence, division, and differentiation be choreographed to produce an efficient therapeutic response? To address this, the effectiveness of different proliferative control strategies on recruitment is assessed at three time points corresponding to short ($T = 3$ days), intermediate ($T = 14$ days), and long times ($T = 28$ days). The parameters q, τ are modulated over a range of physiologically reasonable values and total recruitment R_t is computed at these times. The proliferative restriction n of progenitors is also varied to determine its effect on response dynamics.

The natural proliferation/differentiation tendencies (indicated by the *purple* * in Fig. 2) of progenitors in healthy tissue are clearly not sufficient to mediate repair. At a minimum, the proliferation probability q must be increased to produce a meaningful response, independent of n, τ, or T. For reference in the CNS example, a repair response that raises OLG levels back to a healthy state of ~500 cells/mm^2 (36) would require delivery of $10^4 - 10^5$ cells for a lesion of this size. Additional cell death, which is likely given the inhospitable environment of the lesion, would increase the required number.

We also see that the properties that optimize net recruitment (R_t) depend significantly on the time span of interest. For short times, a significant speedup in the cell cycle progression is required. For long times, the cell cycle length must be decreased, but it is beneficial to maintain some quiescence and not speed things too much. On intermediate time spans, a shorter but possibly nonzero quiescent period is beneficial. The cell cycle length that optimizes recruitment also has significant dependence on the proliferative restriction (n). As a result, there is an intertemporal tradeoff between the strength of early and late time responses, shown in Fig. 3. That is, a cell cycle length that yields a good early response provides a poor late time response and vice versa. We note that spatial stochastic simulations (with $\sigma > 0$) confirm that the addition of random motility does not affect these results substantially as long as $\sigma \sim w$ (see Fig. S1).

Locally confining cell cycle regulation to the lesion mitigates tradeoffs between short and long time responses

The previous analysis indicates there is a tradeoff between short and long time responses. A strong, fast response requires a short cell cycle, whereas a strong long-time response requires a moderate cell cycle length. This however assumes that control of recruitment, cell cycle length, and proliferation probability extend the same distance (r_M) from the lesion. Multiple chemokines are however likely involved in regulating these processes and could potentially have different effects and act at different distances. Alternatively, an individual chemokine could affect these processes in different ways and at different distances.

To investigate the effect of spatially regulating q, τ in different ways, we introduce a spatial range of this regulation ($r_{crit} < r_M$, see Materials and Methods). Five response strategies are simulated (see Materials and Methods) with results reported in Fig. 4 *a*: 1), regulation of q is short range, whereas τ is long range as before (*red*); 2), regulation of τ is short range while q is long range (*blue*); 3), both are short range (*green*). For comparison we also

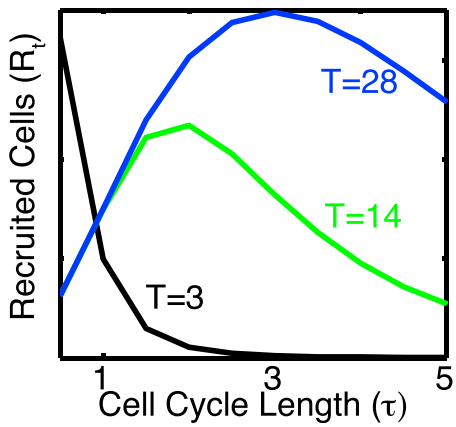

FIGURE 3 Intertemporal tradeoff between early and late time responses. The number of cells recruited to the lesion at times $T = 3$, 14, 28 for $n = 4$ and $q = 1$. $T = 3$ data is scaled by a factor of 10 for visual purposes. All other parameters are the same as in Fig. 2. There is an intertemporal tradeoff, a different cell cycle time is required for efficient recruitment at different times post injury. To see this figure in color, go online.

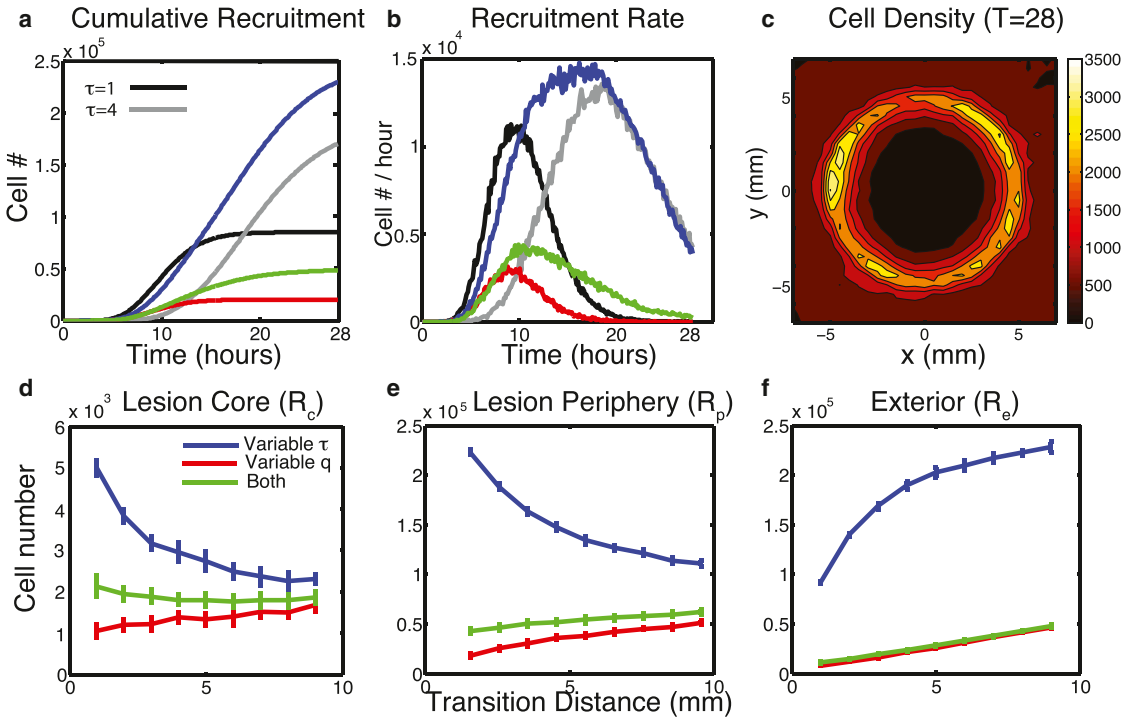

FIGURE 4 Local confinement of cell cycle speedup improves performance and mitigates recruitment tradeoffs. (*Panels a and b*) Time course simulation under five conditions showing cumulative cell recruitment and rate of recruitment. Black curve: $q = 1$ and $\tau = 1$ are independent of chemokine concentration in the chemotactic region A. Gray curve: same as black but with $\tau = 2$. Blue curve: τ has a critical distance of $r_{crit} = 1$ *mm* with $\tau^w = 1$ to τ^h with the range of q extending to r_M. Red curve: q transitions from $q^w = 1$ to q^h at $R_{crit} = 1$ with the range of τ extending to r_M. Green curve: both transition at $R_{crit} = 1$. (*Panel c*) Density of TD cells as a function of space at $T = 28$ days with q independent of chemokine concentration and τ transitioning to $\tau = 1$ at $R_{crit} = 1$ mm. (*Panels d, e, and f*). Delivery efficiency for the three concentration dependent strategies as a function of the critical radius R_{crit}. The number of TDs delivered to the inner core (*d*) of the lesion (defined as the circle of radius 2.5 mm), the periphery (*e*) (the annular region between 2.5 and 5 mm), and outside of the lesion (*f*) (beyond the 5 mm radius lesion) are counted at time $T = 28$. Mean and standard deviation over an ensemble of 50 simulations is reported for each data point. In all cases $w = 0.02$ mm/h is used with $\sigma = w/4$ mm^2/hr, $\tau^h = 9$ days, and $q^h = 0.25$. To see this figure in color, go online.

consider the two best strategies from Fig. 2, *e* and *f*, respectively, with $n = 8$, $q = 1$, and $\tau = 1$ (*black*) or $\tau = 2$ (*gray*). There is a substantial penalty associated with reducing q (Fig. 4, *a* and *b*), independent of the regulatory control of τ, total cell numbers recruited drop substantially as shown by the reduced TD accumulation for the red and green time courses.

There is however substantial benefit to confining cell cycle speedup to the site of damage (*blue trace*, Fig. 4 *a*). Comparing strategies in Fig. 4 *b*, the blue trace nearly matches the intermediate time rate of accumulation of the black trace (*optimal response* at $T = 14$ from Fig. 2 *e*) as well as the late time rate of accumulation of the gray trace (*optimal* $T = 28$ response from Fig. 2 *f*). Furthermore, the time length of high accumulation rate is broader in time with a taller peak rate, and this strategy shows increased TD accumulation above all other strategies beyond ~2 weeks. Thus, locally confining cell cycle regulation near the lesion, although suppressing differentiation well beyond it, increases recruitment. Furthermore, fine control over the spatial extent of cell cycle regulation is not required because improvements in recruitment are monotonic with respect to the effective range of ligands.

Spatially localized cell cycle regulation increases TD infiltration and minimizes wasteful production

The sole goal is not simply to recruit the maximal number of differentiated TD cells possible. Those cells must infiltrate the entire lesion, and it is desirable to avoid wasteful production away from it. Long-range regulation of q and τ leads to poor infiltration of cells to the core (Fig. 4, *c* and *d*). This can be improved by limiting any speedup of the cell cycle to a local region near the site of damage (Fig. 4 *d*, *blue curve*), which increases infiltration. Any speedup of the cell cycle however comes at a price, increased wasteful production of TD cells in healthy tissue (Fig. 4 *f*). This however can also be mitigated by the same strategy. In summary, although careful regulation of proliferation/differentiation (q) is important for tissue maintenance, proper regulation of the cell cycle (τ) is required for a robust damage response.

Random cell motion is required for infiltration of TD cells to the lesion core

The question now becomes, are any of these recruitment strategies sufficient to aid healing. Simulation results for

the strategies that increase recruitment and reduce production beyond the lesion still show poor infiltration of recruited cells to the interior, Fig. 5 *a*. Relative to the peripheral density, there is still poor infiltration. This results from a breakdown of chemotaxis within the lesion. In simulations this is caused by reduced chemoattractant slope, representing loss of signal fidelity due to uniform chemoattractant production, and possibly even receptor saturation at high concentrations.

Infiltration can be improved if the random component of motility σ is comparable to or larger than the chemotactic sensitivity w (Fig. 5, *a–c*). Table 1 however shows that this too comes with a price, reduced total recruitment. For values of $\sigma = w/4, w/2, w$, the number of cells recruited to the core, periphery, and exterior are reported. Increasing the strength of the random component of motion (σ), increases recruitment of cells to the core and exterior, although decreasing recruitment to the periphery. The gain of recruitment to the core does not however offset the loss from the periphery as indicated in the Total column. So as randomness increases, net recruitment falls substantially.

The culprit for this decrease is an increase in the first passage time of any individual cell reaching the lesion as the strength of random motion increases. When chemotactic motion is dominant, passage times are determined primarily by velocity and distance. When random motility dominates, passage times approach that of pure Brownian motion. This has possible implications depending on the particular system of interest. Two is the critical spatial dimension for Brownian motion in the following sense. In one dimension (which in some cases is a reasonable simplification of the spine), the probability of a Brownian particle (e.g., a cell in this context) reaching any point in the domain is one and the expected passage time is finite. Above two dimensions (e.g., the brain), the probability of reaching even a nearby point is zero. In two dimensions the probability of reaching any given point is one, but with infinite expected passage time. So the recruitment penalty associated with increased randomness of motion increases with the effective spatial dimension of the system (even if that dimension is a fractional effective dimension). This suggests different strategies for regulating motility during regeneration in different systems (e.g., the spine versus the brain).

DISCUSSION

Substantial effort has been dedicated to determining the effects of various cytokines and trophic factors on OPC proliferation and differentiation (see McTigue et. al. (9) for an extensive list). Understanding the failure of CNS regeneration and how to overcome it requires determining how these properties are regulated not just in time but also in space. Here, we use a modeling framework to investigate the effectiveness of different strategies for spatially regulating proliferation, differentiation, and chemotaxis of progenitor cells. These results show that spatial heterogeneity of CNS lesions and the need for cell recruitment influence what proliferation/differentiation dynamics lead to an effective regeneration response. In particular, strategies that lead to efficient recruitment of differentiated cells differ from those that are effective in nonspatial settings (18).

Although precise control of proliferation (q) is required for tissue maintenance, it is the cell cycle (τ) that must be properly controlled for an effective regeneration response. Changes in proliferation (q) are of course required, but little precision of that regulation is needed. From a biological point of view, complete removal of premature differentiation is optimal. This requires only removing one of two options (proliferation versus differentiation) rather than precisely balancing the frequency of each. Regulation of the cell cycle on the other hand requires some precision. It is clear that a speedup is necessary. There is however an intertemporal tradeoff associated with this speedup, a fast cell cycle is needed for a good fast response, although an

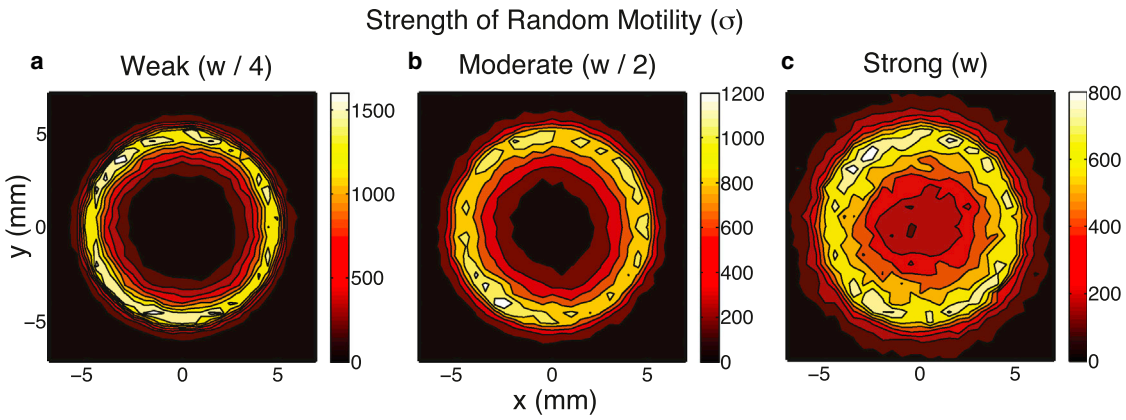

FIGURE 5 Randomness of cell motility improves cell infiltration. Density of TD cells at time $T = 28$ for three values of the diffusion constant σ. It assumed that τ varies between $\tau^h = 9$ and $\tau^w = 1$ days according to (6) with $R_{crit} = 1$ mm. For other parameter, $q^h = 0.25$, $q^w = 1$, $n = 8$, and $w = 0.02$ mm/h. To see this figure in color, go online.

TABLE 1 Increased random cell motility impairs net cell recruitment

Strength of random motility (σ)	No. of cells recruited			
	Core (R_c)	Periphery (R_p)	Total (R_t)	Exterior (R_e)
Weak (w/4)	972	47,622	48,594	24,707
Moderate (w/2)	3003	41,469	44,472	26,784
Strong (w)	5515	34,190	39,705	27,520

Quantification of the effect of random motility on cell recruitment and infiltration. Lineage dynamics are controlled by the optimal strategy shown in Fig. 4 *a*, concentration dependence of τ and independence of q, with all parameters as reported there. An ensemble of 50 simulations for three strengths of random motility (σ) is performed. Recruitment to the core, periphery, and exterior of the lesion are reported with the "Total" column being the sum of core and periphery columns. Mean values, at time $T =$ 28 days, over each ensamble are presented and standard deviations are $<10\%$ in all cases.

intermediate cell cycle length is required for a sustained response. This can be mitigated if cell cycle control is limited to a local region near the lesion, which has additional positive effects of improving infiltration of cells to the interior and limiting wasteful production of differentiated cells in healthy tissue.

These results point to strategies for improving the recruitment response. Specifically, motility, proliferation, and the exit of progenitors from quiescence should be regulated separately and to different spatial extents. Proliferation and chemotaxis should be promoted at longer ranges. This could be accomplished by promoting the production of factors that disperse easily and have a strong effect on proliferation at low concentrations. The G0 phase that OPCs spends extended time in should be substantially shortened or completely removed. This control should however be locally confined to the lesion, which could be accomplished by promoting the production of less dispersive factors that require higher concentrations to be effective.

Unfortunately, even these strategies lead to highly heterogeneous cell recruitment where the lesion core is relatively devoid of cells. This fact is particularly relevant given the known pathology of CNS lesions associated with MS (40), where the same peripheral aggregation is observed. This has been hypothesized to result from impediment of motion by increased cellular density. Our results however show that decreased fidelity of a chemotactic signal near the lesion is an alternative or confounding possibility, consistent with (41). This is made worse by the fact that ~25% of active lesions exhibit an annular ring of activity (i.e., inflammation) (40) around an inactive core. If this region of magnetic resonance imaging enhancement is associated with chemokine production (e.g., TNF-α) (11,14), this would effectively produce a chemotactic wall preventing cells from entering the core of the lesion. One possible solution to this is to increase in randomness of motion, but this is conjecture at this point.

These results make it clear that it is necessary to consider cell lineage dynamics, dynamics of spatial recruitment, and the heterogeneous nature of lesions jointly rather than individually if we are to understand failure of CNS regeneration. This investigation provides an initial step in this direction, but only scratches the surface of the underlying complexity involved. Moving forward requires unraveling the complex feedbacks between progenitors, glial cells (astrocytes in particular), and inflammatory cells that have the potential to both aid and hinder regeneration. Furthermore, it is necessary to understand the role of factors such as inflammation (which is not always associated with demyelination) that affect the environment therapeutic cells are exposed to. Although experimental advancements have and will continue to shed light onto these factors, the inaccessibility of the living CNS necessitates greater involvement of modeling efforts to connect observations from diverse experimental sources to dynamics of living tissue.

SUPPORTING MATERIAL

Two figures, one table, supporting data, and reference (42) are available at http://www.biophysj.org/biophysj/supplemental/S0006-3495(14)00187-8.

We thank Thomas Lane for useful discussions.

This work was supported by National Institutes of Health grants R01GM67247 and P50GM76516 and National Science Foundation grant DMS1161621.

REFERENCES

1. Huseby, E. S., D. Liggitt, …, J. Goverman. 2001. A pathogenic role for myelin-specific CD8(+) T cells in a model for multiple sclerosis. *J. Exp. Med.* 194:669–676.
2. Jurewicz, A., M. Matysiak, …, K. Selmaj. 2005. Tumour necrosis factor-induced death of adult human oligodendrocytes is mediated by apoptosis inducing factor. *Brain.* 128:2675–2688.
3. Juurlink, B. H. 1997. Response of glial cells to ischemia: roles of reactive oxygen species and glutathione. *Neurosci. Biobehav. Rev.* 21:151–166.
4. Barres, B. A., and M. C. Raff. 1999. Axonal control of oligodendrocyte development. *J. Cell Biol.* 147:1123–1128.
5. Wilkins, A., S. Chandran, and A. Compston. 2001. A role for oligodendrocyte-derived IGF-1 in trophic support of cortical neurons. *Glia.* 36:48–57.
6. Bruck, W., T. Kuhlmann, and C. Stadelmann. 2003. Remyelination in multiple sclerosis. *J. Neurol. Sci.* 206:181–185.
7. Fancy, S. P., M. R. Kotter, …, R. J. Franklin. 2010. Overcoming remyelination failure in multiple sclerosis and other myelin disorders. *Exp. Neurol.* 225:18–23.
8. Pluchino, S., L. Zanotti, …, G. Martino. 2009. Regeneration and repair in multiple sclerosis: the role of cell transplantation. *Neurosci. Lett.* 456:101–106.
9. McTigue, D. M., and R. B. Tripathi. 2008. The life, death, and replacement of oligodendrocytes in the adult CNS. *J. Neurochem.* 107:1–19.
10. Du, Y., and C. F. Dreyfus. 2002. Oligodendrocytes as providers of growth factors. *J. Neurosci. Res.* 68:647–654.
11. Patel, J. R., J. L. Williams, …, R. S. Klein. 2012. Astrocyte TNFR2 is required for CXCL12-mediated regulation of oligodendrocyte progenitor proliferation and differentiation within the adult CNS. *Acta*

Neuropathol. 124:847–860. http://dx.doi.org/10.1007/s00401–012–1034–0.

12. Patel, J. R., E. E. McCandless, …, R. S. Klein. 2010. Cxcr4 promotes differentiation of oligodendrocyte progenitors and remyelination. *Proc. Natl. Acad. Sci. USA.* 107:11062–11067.
13. Banisadr, G., T. J. Frederick, …, R. J. Miller. 2011. The role of CXCR4 signaling in the migration of transplanted oligodendrocyte progenitors into the cerebral white matter. *Neurobiol. Dis.* 44:19–27.
14. Carbajal, K. S., C. Schaumburg, …, T. E. Lane. 2010. Migration of engrafted neural stem cells is mediated by CXCL12 signaling through CXCR4 in a viral model of multiple sclerosis. *Proc. Natl. Acad. Sci. USA.* 107:11068–11073.
15. Franklin, R. J., and W. F. Blakemore. 1997. To what extent is oligodendrocyte progenitor migration a limiting factor in the remyelination of multiple sclerosis lesions? *Mult. Scler.* 3:84–87.
16. Hartman, N. W., J. E. Carpentino, …, L. Grabel. 2010. CXCL12-mediated guidance of migrating embryonic stem cell-derived neural progenitors transplanted into the hippocampus. *PLoS ONE.* 5:e15856.
17. Bocharov, G., J. Quiel, …, Z. Grossman. 2011. Feedback regulation of proliferation vs. differentiation rates explains the dependence of CD4 T-cell expansion on precursor number. *Proc. Natl. Acad. Sci. USA.* 108:3318–3323.
18. Lander, A. D., K. K. Gokoffski, …, A. L. Calof. 2009. Cell lineages and the logic of proliferative control. *PLoS Biol.* 7:e15.
19. Lo, W. C., C.-S. Chou, …, Q. Nie. 2009. Feedback regulation in multistage cell lineages. *Math. Biosci. Eng.* 6:59–82.
20. Mangel, M., and M. B. Bonsall. 2013. Stem cell biology is population biology: differentiation of hematopoietic multipotent progenitors to common lymphoid and myeloid progenitors. *Theor. Biol. Med. Model.* 10:5.
21. Marciniak-Czochra, A., T. Stiehl, …, W. Wagner. 2009. Modeling of asymmetric cell division in hematopoietic stem cells—regulation of self-renewal is essential for efficient repopulation. *Stem Cells Dev.* 18:377–385.
22. Hu, G. M., C. Y. Lee, …, W. J. Tzeng. 2012. Mathematical model of heterogeneous cancer growth with an autocrine signalling pathway. *Cell Prolif.* 45:445–455.
23. MacKey, M. C. 2001. Cell kinetic status of haematopoietic stem cells. *Cell Prolif.* 34:71–83.
24. Traulsen, A., T. Lenaerts, …, D. Dingli. 2013. On the dynamics of neutral mutations in a mathematical model for a homogeneous stem cell population. *J. R. Soc. Interface.* 10:20120810.
25. Cumming, B. D., D. L. McElwain, and Z. Upton. 2010. A mathematical model of wound healing and subsequent scarring. *J. R. Soc. Interface.* 7:19–34.
26. Menon, S. N., J. A. Flegg, …, D. L. McElwain. 2012. Modelling the interaction of keratinocytes and fibroblasts during normal and abnormal wound healing processes. *Proc. Biol. Sci.* 279:3329–3338.
27. Xue, C., A. Friedman, and C. K. Sen. 2009. A mathematical model of ischemic cutaneous wounds. *Proc. Natl. Acad. Sci. USA.* 106:16782–16787.
28. Blagoev, K. B. 2011. Organ aging and susceptibility to cancer may be related to the geometry of the stem cell niche. *Proc. Natl. Acad. Sci. USA.* 108:19216–19221.
29. Rodriguez-Brenes, I. A., D. Wodarz, and N. L. Komarova. 2013. Stem cell control, oscillations and tissue regeneration in spatial and non-spatial models. *Fron. Oncol.* 3:82.
30. Chou, C.-S., W.-C. Lo, …, Q. Nie. 2010. Spatial dynamics of multistage cell lineages in tissue stratification. *Biophys. J.* 99:3145–3154.
31. Ovadia, J., and Q. Nie. 2013. Stem cell niche structure as an inherent cause of undulating epithelial morphologies. *Biophys. J.* 104:237–246.
32. Barres, B. A., M. A. Lazar, and M. C. Raff. 1994. A novel role for thyroid hormone, glucocorticoids and retinoic acid in timing oligodendrocyte development. *Development.* 120:1097–1108.
33. Temple, S., and M. C. Raff. 1986. Clonal analysis of oligodendrocyte development in culture: evidence for a developmental clock that counts cell divisions. *Cell.* 44:773–779.
34. Imitola, J., K. Raddassi, …, S. J. Khoury. 2004. Directed migration of neural stem cells to sites of CNS injury by the stromal cell-derived factor 1alpha/CXC chemokine receptor 4 pathway. *Proc. Natl. Acad. Sci. USA.* 101:18117–18122.
35. Gillespie, D. T. 1977. Exact stochastic simulation of coupled chemical reactions. *J. Phys. Chem.* 81:2340–2361.
36. Carbajal, K. S., J. L. Miranda, …, T. E. Lane. 2011. CXCR4 signaling regulates remyelination by endogenous oligodendrocyte progenitor cells in a viral model of demyelination. *Glia.* 59:1813–1821.
37. Scholzen, T., and J. Gerdes. 2000. The Ki-67 protein: from the known and the unknown. *J. Cell. Physiol.* 182:311–322.
38. Hughes, E. G., S. H. Kang, …, D. E. Bergles. 2013. Oligodendrocyte progenitors balance growth with self-repulsion to achieve homeostasis in the adult brain. *Nat. Neurosci.* 16:668–676.
39. Wolswijk, G., and M. Noble. 1989. Identification of an adult-specific glial progenitor cell. *Development.* 105:387–400.
40. He, J., R. I. Grossman, …, L. J. Mannon. 2001. Enhancing patterns in multiple sclerosis: evolution and persistence. *AJNR Am. J. Neuroradiol.* 22:664–669.
41. Sabelström, H., M. Stenudd, …, J. Frisén. 2013. Resident neural stem cells restrict tissue damage and neuronal loss after spinal cord injury in mice. *Science.* 342:637–640.
42. Rafaksjum, V. A., and M. Noble. 1989. Identification of an adult-specific glial progenitor cell. *Development.* 105:387–400.